

Charged Multiplicities in Z Decays into u, d, and s Quarks

The OPAL Collaboration

Abstract

About 4.4 million hadronic decays of Z bosons, recorded by the OPAL detector at LEP at a centre-of-mass energy of around $\sqrt{s} = 91.2 \text{ GeV}$, are used to determine the mean charged particle multiplicities for the three light quark flavours. Events from primary u, d, and s quarks are tagged by selecting characteristic particles which carry a large fraction of the beam energy. The charged particle multiplicities are measured in the hemispheres opposite to these particles. An unfolding procedure is applied to obtain these multiplicities for each primary light quark flavour. This yields

$$\langle n_u \rangle = 17.77 \pm 0.51^{+0.86}_{-1.20}, \quad \langle n_d \rangle = 21.44 \pm 0.63^{+1.46}_{-1.17}, \quad \langle n_s \rangle = 20.02 \pm 0.13^{+0.39}_{-0.37},$$

where statistical and systematic errors are given. The results for $\langle n_u \rangle$ and $\langle n_d \rangle$ are almost fully statistically anti-correlated. Within the errors the result is consistent with the flavour independence of the strong interaction for the particle multiplicities in events from the light up, down, and strange quarks.

(Submitted to European Physical Journal C)

The OPAL Collaboration

G. Abbiendi², C. Ainsley⁵, P.F. Åkesson³, G. Alexander²², J. Allison¹⁶, G. Anagnostou¹, K.J. Anderson⁹, S. Arcelli¹⁷, S. Asai²³, D. Axen²⁷, G. Azuelos^{18,a}, I. Bailey²⁶, A.H. Ball⁸, E. Barberio⁸, R.J. Barlow¹⁶, T. Behnke²⁵, K.W. Bell²⁰, G. Bella²², A. Bellerive⁹, G. Benelli², S. Bentvelsen⁸, S. Bethke³², O. Biebel³², I.J. Bloodworth¹, O. Boeriu¹⁰, P. Bock¹¹, J. Böhme^{14,g}, D. Bonacorsi², M. Boutemur³¹, S. Braibant⁸, P. Bright-Thomas¹, L. Brigliadori², R.M. Brown²⁰, H.J. Burckhart⁸, J. Cammin³, P. Capiluppi², R.K. Carnegie⁶, B. Caron²⁸, A.A. Carter¹³, J.R. Carter⁵, C.Y. Chang¹⁷, D.G. Charlton^{1,b}, P.E.L. Clarke¹⁵, E. Clay¹⁵, I. Cohen²², O.C. Cooke⁸, J. Couchman¹⁵, R.L. Coxe⁹, A. Csilling^{15,i}, M. Cuffiani², S. Dado²¹, G.M. Dallavalle², S. Dallison¹⁶, A. De Roeck⁸, E.A. De Wolf⁸, P. Dervan¹⁵, K. Desch²⁵, B. Dienes^{30,f}, M.S. Dixit⁷, M. Donkers⁶, J. Dubbert³¹, E. Duchovni²⁴, G. Duckeck³¹, I.P. Duerdoth¹⁶, P.G. Estabrooks⁶, E. Etzion²², F. Fabbri², M. Fanti², L. Feld¹⁰, P. Ferrari¹², F. Fiedler⁸, I. Fleck¹⁰, M. Ford⁵, A. Frey⁸, A. Fürtjes⁸, D.I. Futyan¹⁶, P. Gagnon¹², J.W. Gary⁴, G. Gaycken²⁵, C. Geich-Gimbel³, G. Giacomelli², P. Giacomelli⁸, D. Glenzinski⁹, J. Goldberg²¹, C. Grandi², K. Graham²⁶, E. Gross²⁴, J. Grunhaus²², M. Gruwé²⁵, P.O. Günther³, C. Hajdu²⁹, G.G. Hanson¹², K. Harder²⁵, A. Harel²¹, M. Harin-Dirac⁴, M. Hauschild⁸, C.M. Hawkes¹, R. Hawkings⁸, R.J. Hemingway⁶, C. Hensel²⁵, G. Herten¹⁰, R.D. Heuer²⁵, J.C. Hill⁵, A. Hocker⁹, K. Hoffman⁸, R.J. Homer¹, A.K. Honma⁸, D. Horváth^{29,c}, K.R. Hossain²⁸, R. Howard²⁷, P. Hüntemeyer²⁵, P. Igo-Kemenes¹¹, K. Ishii²³, F.R. Jacob²⁰, A. Jawahery¹⁷, H. Jeremie¹⁸, C.R. Jones⁵, P. Jovanovic¹, T.R. Junk⁶, N. Kanaya²³, J. Kanzaki²³, G. Karapetian¹⁸, D. Karlen⁶, V. Kartvelishvili¹⁶, K. Kawagoe²³, T. Kawamoto²³, R.K. Keeler²⁶, R.G. Kellogg¹⁷, B.W. Kennedy²⁰, D.H. Kim¹⁹, K. Klein¹¹, A. Klier²⁴, S. Kluth³², T. Kobayashi²³, M. Kobel³, T.P. Kokott³, S. Komamiya²³, R.V. Kowalewski²⁶, T. Kress⁴, P. Krieger⁶, J. von Krogh¹¹, D. Krop¹², T. Kuhl³, M. Kupper²⁴, P. Kyberd¹³, G.D. Lafferty¹⁶, H. Landsman²¹, D. Lanske¹⁴, I. Lawson²⁶, J.G. Layter⁴, A. Leins³¹, D. Lellouch²⁴, J. Letts¹², L. Levinson²⁴, R. Liebisch¹¹, J. Lillich¹⁰, C. Littlewood⁵, A.W. Lloyd¹, S.L. Lloyd¹³, F.K. Loebinger¹⁶, G.D. Long²⁶, M.J. Losty⁷, J. Lu²⁷, J. Ludwig¹⁰, A. Macchiolo¹⁸, A. Macpherson^{28,l}, W. Mader³, S. Marcellini², T.E. Marchant¹⁶, A.J. Martin¹³, J.P. Martin¹⁸, G. Martinez¹⁷, T. Mashimo²³, P. Mättig²⁴, W.J. McDonald²⁸, J. McKenna²⁷, T.J. McMahon¹, R.A. McPherson²⁶, F. Meijers⁸, P. Mendez-Lorenzo³¹, W. Menges²⁵, F.S. Merritt⁹, H. Mes⁷, A. Michelini², S. Mihara²³, G. Mikenberg²⁴, D.J. Miller¹⁵, W. Mohr¹⁰, A. Montanari², T. Mori²³, K. Nagai¹³, I. Nakamura²³, H.A. Neal³³, R. Nisius⁸, S.W. O’Neale¹, F.G. Oakham⁷, F. Odorici², A. Oh⁸, A. Okpara¹¹, M.J. Oreglia⁹, S. Orito²³, G. Pásztor^{8,i}, J.R. Pater¹⁶, G.N. Patrick²⁰, P. Pfeifenschneider^{14,h}, J.E. Pilcher⁹, J. Pinfold²⁸, D.E. Plane⁸, B. Poli², J. Polok⁸, O. Pooth⁸, M. Przybycień^{8,d}, A. Quadt⁸, K. Rabbertz⁸, C. Rembser⁸, P. Renkel²⁴, H. Rick⁴, N. Rodning²⁸, J.M. Roney²⁶, S. Rosati³, K. Roscoe¹⁶, A.M. Rossi², Y. Rozen²¹, K. Runge¹⁰, O. Runolfsson⁸, D.R. Rust¹², K. Sachs⁶, T. Saeki²³, O. Sahr³¹, E.K.G. Sarkisyan^{8,m}, C. Sbarra²⁶, A.D. Schaile³¹, O. Schaile³¹, P. Scharff-Hansen⁸, M. Schröder⁸, M. Schumacher²⁵, C. Schwick⁸, W.G. Scott²⁰, R. Seuster^{14,g}, T.G. Shears^{8,j}, B.C. Shen⁴, C.H. Shepherd-Themistocleous⁵, P. Sherwood¹⁵, G.P. Siroli², A. Skuja¹⁷, A.M. Smith⁸, G.A. Snow¹⁷, R. Sobie²⁶, S. Söldner-Rembold^{10,e}, S. Spagnolo²⁰, M. Sproston²⁰, A. Stahl³, K. Stephens¹⁶, K. Stoll¹⁰, D. Strom¹⁹, R. Ströhmer³¹, L. Stumpf²⁶, B. Surrow⁸, S.D. Talbot¹, S. Tarem²¹, R.J. Taylor¹⁵, R. Teuscher⁹,

J. Thomas¹⁵, M.A. Thomson⁸, M. Tönnemann³², E. Torrence⁹, S. Towers⁶, D. Toya²³,
T. Trefzger³¹, I. Trigger⁸, Z. Trócsányi^{30,f}, E. Tsur²², M.F. Turner-Watson¹, I. Ueda²³,
B. Vachon²⁶, P. Vannerem¹⁰, M. Verzocchi⁸, H. Voss⁸, J. Vossebeld⁸, D. Waller⁶,
C.P. Ward⁵, D.R. Ward⁵, P.M. Watkins¹, A.T. Watson¹, N.K. Watson¹, P.S. Wells⁸,
T. Wengler⁸, N. Wermes³, D. Wetterling¹¹, J.S. White⁶, G.W. Wilson¹⁶, J.A. Wilson¹,
T.R. Wyatt¹⁶, S. Yamashita²³, V. Zacek¹⁸, D. Zer-Zion^{8,k}

¹School of Physics and Astronomy, University of Birmingham, Birmingham B15 2TT, UK

²Dipartimento di Fisica dell' Università di Bologna and INFN, I-40126 Bologna, Italy

³Physikalisches Institut, Universität Bonn, D-53115 Bonn, Germany

⁴Department of Physics, University of California, Riverside CA 92521, USA

⁵Cavendish Laboratory, Cambridge CB3 0HE, UK

⁶Ottawa-Carleton Institute for Physics, Department of Physics, Carleton University, Ottawa, Ontario K1S 5B6, Canada

⁷Centre for Research in Particle Physics, Carleton University, Ottawa, Ontario K1S 5B6, Canada

⁸CERN, European Organisation for Nuclear Research, CH-1211 Geneva 23, Switzerland

⁹Enrico Fermi Institute and Department of Physics, University of Chicago, Chicago IL 60637, USA

¹⁰Fakultät für Physik, Albert Ludwigs Universität, D-79104 Freiburg, Germany

¹¹Physikalisches Institut, Universität Heidelberg, D-69120 Heidelberg, Germany

¹²Indiana University, Department of Physics, Swain Hall West 117, Bloomington IN 47405, USA

¹³Queen Mary and Westfield College, University of London, London E1 4NS, UK

¹⁴Technische Hochschule Aachen, III Physikalisches Institut, Sommerfeldstrasse 26-28, D-52056 Aachen, Germany

¹⁵University College London, London WC1E 6BT, UK

¹⁶Department of Physics, Schuster Laboratory, The University, Manchester M13 9PL, UK

¹⁷Department of Physics, University of Maryland, College Park, MD 20742, USA

¹⁸Laboratoire de Physique Nucléaire, Université de Montréal, Montréal, Quebec H3C 3J7, Canada

¹⁹University of Oregon, Department of Physics, Eugene OR 97403, USA

²⁰CLRC Rutherford Appleton Laboratory, Chilton, Didcot, Oxfordshire OX11 0QX, UK

²¹Department of Physics, Technion-Israel Institute of Technology, Haifa 32000, Israel

²²Department of Physics and Astronomy, Tel Aviv University, Tel Aviv 69978, Israel

²³International Centre for Elementary Particle Physics and Department of Physics, University of Tokyo, Tokyo 113-0033, and Kobe University, Kobe 657-8501, Japan

²⁴Particle Physics Department, Weizmann Institute of Science, Rehovot 76100, Israel

²⁵Universität Hamburg/DESY, II Institut für Experimental Physik, Notkestrasse 85, D-22607 Hamburg, Germany

²⁶University of Victoria, Department of Physics, P O Box 3055, Victoria BC V8W 3P6, Canada

²⁷University of British Columbia, Department of Physics, Vancouver BC V6T 1Z1, Canada

²⁸University of Alberta, Department of Physics, Edmonton AB T6G 2J1, Canada

²⁹Research Institute for Particle and Nuclear Physics, H-1525 Budapest, P O Box 49, Hungary

³⁰Institute of Nuclear Research, H-4001 Debrecen, P O Box 51, Hungary

³¹Ludwigs-Maximilians-Universität München, Sektion Physik, Am Coulombwall 1, D-85748 Garching, Germany

³²Max-Planck-Institute für Physik, Föhring Ring 6, 80805 München, Germany

³³Yale University, Department of Physics, New Haven, CT 06520, USA

^a and at TRIUMF, Vancouver, Canada V6T 2A3

^b and Royal Society University Research Fellow

^c and Institute of Nuclear Research, Debrecen, Hungary

^d and University of Mining and Metallurgy, Cracow

^e and Heisenberg Fellow

^f and Department of Experimental Physics, Lajos Kossuth University, Debrecen, Hungary

^g and MPI München

^h now at MPI für Physik, 80805 München

ⁱ and Research Institute for Particle and Nuclear Physics, Budapest, Hungary

^j now at University of Liverpool, Dept of Physics, Liverpool L69 3BX, UK

^k and University of California, Riverside, High Energy Physics Group, CA 92521, USA

^l and CERN, EP Div, 1211 Geneva 23

^m and Tel Aviv University, School of Physics and Astronomy, Tel Aviv 69978, Israel.

1 Introduction

The flavour independence of the strong coupling is a fundamental property of quantum chromodynamics (QCD). A breaking of the flavour symmetry should only occur due to calculable mass effects. These mass effects have been observed for bottom quarks [1, 2] using event shapes and jet rates in the final state of electron-positron annihilation into $b\bar{b}$. Another observable which can be employed to test flavour independence is the multiplicity of charged hadrons in jets originating from quarks of a specific flavour. According to the local parton hadron duality hypothesis (LPHD) [3], the particle multiplicity is related to the gluon multiplicity inside a jet which depends on the value of the strong coupling constant [4]. A dependence of the multiplicity of charged hadrons on the quark flavour has been found for heavy quarks [5]. Up to now only few measurements exist on the flavour independence of the strong interaction in the light quark sector (up, down, strange quarks) [2]. Within the large uncertainties due to the limited statistics, flavour independence of the strong interaction is supported.

This paper presents a new, high statistics investigation of the flavour dependence of the strong interaction. It is based on the mean charged multiplicity determined separately for events of primary up, down, and strange quarks in e^+e^- annihilation at centre-of-mass energies close to the mass of the Z boson. To identify the flavour of the primary quark in the Z decay, the leading particle effect is exploited [6]. This assumption of a correlation between the flavour of the primary quark and the type of the hadron carrying the largest

momentum has recently received further support by measurements of the SLD [7] and OPAL collaborations [8].

The study presented in this paper uses three different selections of events with leading K_S^0 and K^\pm mesons, and highly energetic stable charged particles, denoted “high x_E ” in the following. Due to the different fractions of primary up, down, and strange quarks in these samples a statistical decomposition of the contributions from each of the three quark flavours is possible. The leading K_S^0 and K^\pm meson selections, even though dominantly stemming from primary strange quarks, yield the separation of up and down quark events since a leading K_S^0 (K^\pm) meson is rarely formed from a primary up (down) quark while both K_S^0 and K^\pm are equally likely to be produced in a strange quark event. Together with the high x_E selection, containing up, down, and strange quark events in approximately equal proportions, properties like the mean charged particle multiplicity in events of each of these three light quark flavours can be determined by statistical unfolding. The mean charged multiplicity is determined from all long-lived charged particles in the hemisphere opposite to the leading particle where the two hemispheres of an event are defined by the plane perpendicular to the thrust axis which contains the main interaction point. Choosing the opposite hemisphere minimizes the bias of the measured multiplicity due to the high energy of the leading particle.

Before the three selections of leading particles are presented in Section 3, the OPAL detector and the data samples used for this study are briefly introduced in Section 2. The determination of the charged particle multiplicities is discussed in Section 4. The investigation of various sources of systematic uncertainty is detailed in Section 5. Section 6 presents a cross-check of the analysis using flavour fractions obtained from the data. The results of this analysis are presented in Section 7.

2 The OPAL detector, data, and Monte Carlo simulation

The OPAL detector has been described in detail elsewhere [9]. The analysis presented here relies mainly on the reconstruction of charged particles in the large volume jet chamber whose performance has been presented in [10]. A solenoidal coil surrounds all tracking detectors. It provides a field of 0.435 T along the beam axis¹. Tracks of charged particles are reconstructed with up to 159 space points. Their momenta in the plane transverse to the beam-axis, p_{xy} , can be determined to a precision of $\sigma_{p_{xy}}/p_{xy} = \sqrt{0.02^2 + (p_{xy} \cdot 0.0015/\text{GeV})^2}$. This resolution degrades towards the acceptance boundary of $|\cos\theta| \approx 0.98$. From the specific energy loss dE/dx , which is measured from up to 159 samples with a resolution of $\sigma(dE/dx)/(dE/dx) \approx 0.035$, the type of the charged particle can be identified over a wide momentum range.

The analysis is based on data recorded with the OPAL detector between 1990 and

¹The coordinate system of OPAL has the z axis along the electron beam direction, the y axis points upwards and x towards the centre of the LEP ring. The polar angle θ is measured with respect to the z axis.

1995 comprising about 4.4 million hadronic events at centre-of-mass energies \sqrt{s} around 91.2 GeV (LEP I). The events considered for this study were preselected by a standard selection for high multiplicity events [11] which relies on a minimum number of measured tracks of charged particles in the tracking detectors and clusters of energy deposited in the electromagnetic calorimeter. The remaining background of two-photon processes and τ -pair events are estimated to be 0.07 % and 0.11 %, respectively.

Tracks to be used for the reconstruction or identification of the leading particles and for the determination of the charged multiplicity were required to pass the quality selection cuts as detailed in [12]. These tracks had to have at least 20 hits in the jet chamber and a closest approach to the interaction point in the plane perpendicular to the beam axis of $|d_0| < 5$ cm. The track momenta had to be between 0.1 and 65 GeV. Events with τ -pairs are further suppressed by requiring at least seven tracks.

The Monte Carlo simulation comprised about 8.5 million hadronic events simulated by version 7.4 of the JETSET program [13] which has been tuned to describe the OPAL data [14]. The generated events were passed through a detailed simulation of the OPAL detector [15] and processed using the same reconstruction and selection algorithm as the measured data.

3 Selection of flavour enriched data samples

Every event is divided into two hemispheres by the plane perpendicular to the thrust axis containing the interaction point. In each hemisphere we searched for K_S^0 and K^\pm mesons, and highly energetic stable charged particles, whose energy fraction $x_E = 2E/\sqrt{s}$ is above a certain threshold. Due to the cuts, in particular on x_E , these three samples are enriched in events from up, down, and strange quarks in different proportions (see Table 1). The x_E selection cuts were chosen to have samples of comparable size.

3.1 K_S^0 selection

K_S^0 mesons were selected via their decay into two charged pions using the procedure described in [16]. It was adapted for large momenta of the K_S^0 mesons by dropping the specific d_0 cut imposed on the two pions in the default procedure. Any two oppositely charged particles were combined. The invariant mass $m_{\pi\pi}$ was calculated assuming the pion mass for the particles. K_S^0 candidates were required to have $|m_{K_S^0} - m_{\pi\pi}| < 60$ MeV using the mass of a K_S^0 meson, $m_{K_S^0}$, given in [17]. Photon conversions were rejected by demanding $m_{ee} > 100$ MeV if the electron mass is assigned to both tracks. The impact of detector effects close to the acceptance boundary is reduced by restricting the polar angle of K_S^0 candidates to $|\cos\theta| < 0.9$. To enrich the sample in primary strange and down quarks and to suppress up, charm, and bottom events, a requirement on the scaled energy of the K_S^0 candidate of $x_E > 0.4$ was applied. Candidates with $x_E > 1.07$ were rejected. This takes into account the 7 % momentum resolution for particles with the beam energy.

| | tag | K_S^0 | K^\pm | high x_E |
|------------------------|--------------------------------|-----------------|-----------------|-----------------|
| | x_E range | 0.40-1.07 | 0.50-1.07 | 0.70-1.07 |
| Data | $N^{\text{tag}} =$ | 19359 \pm 139 | 18979 \pm 138 | 27909 \pm 167 |
| MC expectation | $N_{\text{MC}}^{\text{tag}} =$ | 19303 \pm 99 | 18947 \pm 99 | 27845 \pm 119 |
| u fraction $[10^{-2}]$ | $f_u^{\text{tag}} =$ | 8.3 \pm 0.1 | 21.7 \pm 0.2 | 31.4 \pm 0.2 |
| d fraction $[10^{-2}]$ | $f_d^{\text{tag}} =$ | 15.6 \pm 0.2 | 13.9 \pm 0.2 | 27.8 \pm 0.2 |
| s fraction $[10^{-2}]$ | $f_s^{\text{tag}} =$ | 57.0 \pm 0.3 | 53.1 \pm 0.3 | 36.4 \pm 0.2 |
| c fraction $[10^{-2}]$ | $f_c^{\text{tag}} =$ | 14.6 \pm 0.2 | 9.0 \pm 0.2 | 3.0 \pm 0.1 |
| b fraction $[10^{-2}]$ | $f_b^{\text{tag}} =$ | 4.5 \pm 0.1 | 2.3 \pm 0.1 | 1.4 \pm 0.1 |

Table 1: Number of tagged hemispheres in data and in the Monte Carlo simulation, scaled to the same integrated luminosity, and the flavour composition of the three samples found from the simulation after applying the reweighting procedure described in Section 3.4. The errors are statistical only.

Figure 1 (a) and (d) show the energy spectrum of the K_S^0 candidates and the expected flavour composition of the events tagged by the K_S^0 candidates. Table 1 gives the number of tagged hemispheres in the data as well as the expected number and the flavour composition of the sample taken from the Monte Carlo simulation plus their statistical errors. The sizeable charm quark contribution is due to D mesons decaying into K_S^0 .

3.2 K^\pm selection

Charged kaons were identified using the energy loss measurements in the jet chamber [10]. To effectively reject the contribution of charged pions and protons, only tracks in the central region of the jet chamber, $|\cos\theta| < 0.72$, were considered which have at least 130 hits for the momentum measurement and a minimum of 100 hits for the determination of the energy loss. Tracks azimuthally closer than 0.5° to an anode wire plane of the jet chamber were not accepted to avoid biases from the significantly degraded resolution of both momentum and energy loss measurement close to these planes.

Each track is assigned five dE/dx weights, w_h , calculated from the probabilities of the measured energy loss of the track to be consistent with that expected for a particle of type h , where h can be $p(\bar{p})$, K^\pm , π^\pm , μ^\pm or e^\pm . The weight is positive signed if $dE/dx(\text{measured}) > dE/dx(\text{expected})$ according to a particular hypothesis, and negative otherwise. K^\pm were selected by requiring:

$$\begin{aligned}
|w_K| &> \max(|w_p|, |w_\pi|, |w_\mu|, |w_e|) \\
|w_K| &> 0.1 \\
\text{and } |w_\pi| &< 0.1
\end{aligned}$$

This yielded, according to the simulation, a composition of the sample of tagged particles of about 77 % kaons, 13 % pions, and 9.5 % protons. The remainder is due to muons and charged hyperons. It was not attempted to correct the K^\pm selection for the pion and proton contributions directly.

OPAL

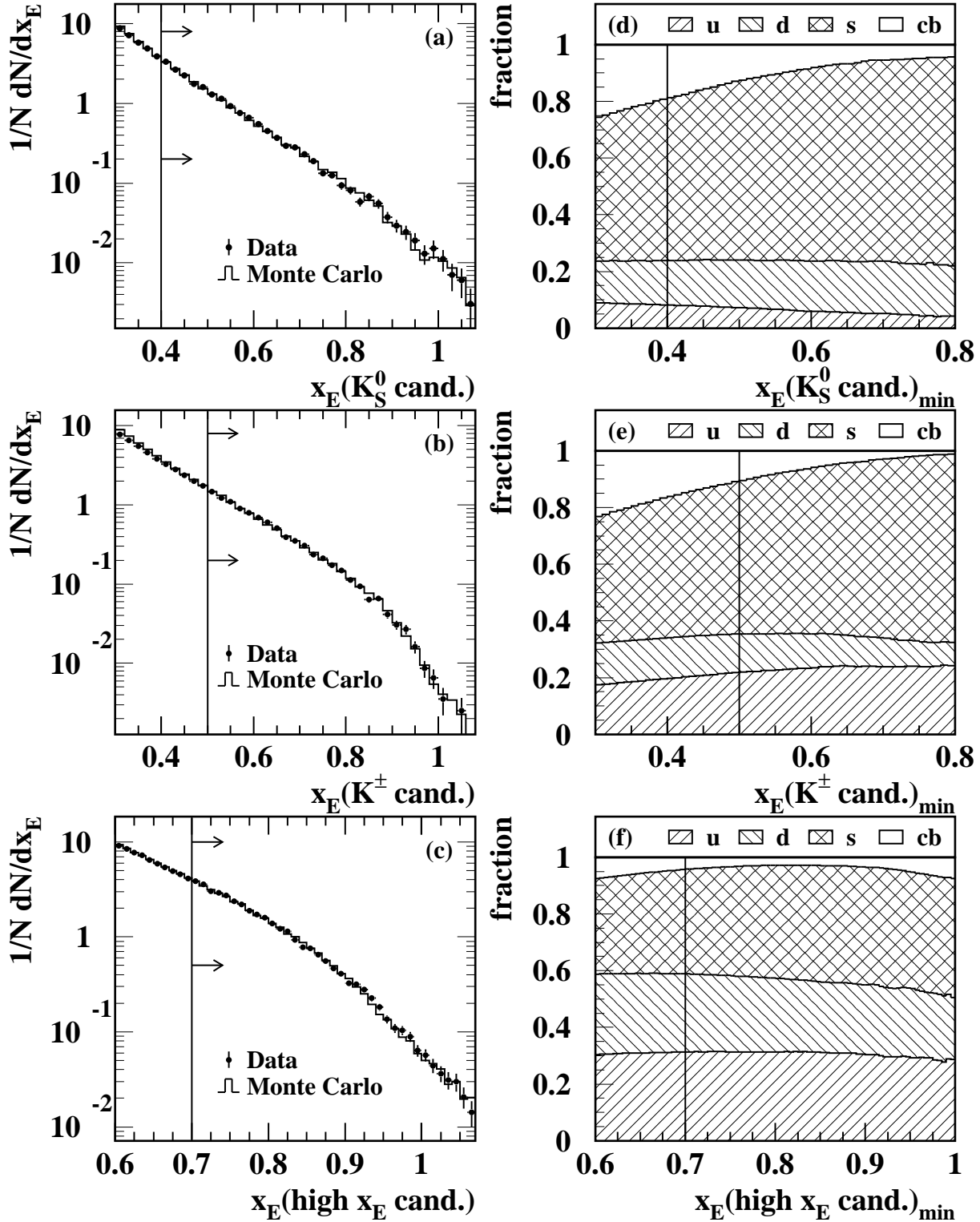


Figure 1: (a)-(c) Observed energy spectra of K_S^0 , K^\pm , and high x_E candidates. The solid line shows the Monte Carlo simulation normalized to the integrated luminosity of the data after applying the reweighting procedure described in Section 3.4. (d)-(f) Corresponding flavour fractions taken from the Monte Carlo simulation as a function of the cut on the minimum energy fraction, $x_{E,\min}$, of the tag particle. The x_E cuts chosen for the flavour enriched samples are indicated by the vertical lines.

Figure 1 (b) shows the energy spectrum of the K^\pm candidates. To enrich the sample in events of primary strange and up quarks, a cut on the minimum scaled energy of $x_E > 0.5$ was applied as shown in Figure 1 (e). Badly reconstructed tracks were rejected by requiring $x_E < 1.07$. Table 1 summarizes the number of tagged hemispheres, the expected number and the primary flavour composition taken from the Monte Carlo simulation.

3.3 High x_E particle selection

Even though the fragmentation of bottom and charm quarks is harder than that of the light quarks, the cascade decays of the b- and c-hadrons lead to many stable particles which consequently have a significantly softer energy spectrum. Thus the selection of stable charged particles carrying a high energy fraction x_E , calculated using the assumption that the particle is a pion, depletes an event sample of primary charm and bottom quarks. Besides the cuts on the scaled energy of $0.7 < x_E < 1.07$, additional cuts concerned the selection of well-reconstructed tracks which were required to have at least 130 hits used for the reconstruction, a polar angle of $|\cos \theta| < 0.72$ and an azimuthal angular distance from the closest anode wire plane of at least 0.5° . Moreover, the $\chi^2_{r\varphi}$ per degree of freedom of the fit of the track to the hits in the plane perpendicular to the beam axis had to be less than 2. This tight cut rejected badly reconstructed tracks, including those containing kinks due to an unrecognized decay in flight.

The energy spectrum of the high x_E candidates and the flavour composition depending on the cut on the minimum energy of the high x_E particles are shown in Figures 1 (c) and (f). The slightly rising fraction of heavy quark events at very large x_E is due to the remaining contribution of badly reconstructed tracks in this energy region. Such tracks occur with the same low probability for each primary flavour.

In Table 1 the number of tagged hemispheres found in the data are given and compared with the expected number from the simulation. It should be pointed out that about 10% of the high x_E hemispheres are also selected with the K^\pm selection cuts. No rejection was applied, but it was checked that eliminating the 10% had no significant effect on the result of this analysis. The small statistical correlation was taken into account.

3.4 Checks of the flavour composition

A crucial ingredient in this analysis is the knowledge of the flavour composition of the three tagged event samples. The JETSET Monte Carlo simulation using the tuned parameters of [14] predicts for each of the tagged particles in the region of high values of x_E a larger differential cross-section $(1/N) \cdot (dN/dx_E)$ than measured in the data. This discrepancy was accounted for by applying a flavour independent reweighting to each of the three tagged event samples in the simulation. The reweighting factors were derived from the ratio of the x_E spectra of the tagged particles in the data and the simulation. They were parametrized by a function $f(x_E) = c \cdot (1 - x_E)^\delta$ whose form is motivated by the Lund symmetric fragmentation function [18]. Each tag type had its own reweighting function,

| (a) | | N^{tag} | K_S^0 | K^\pm | high x_E |
|------------|------|------------------|------------|--------------|--------------|
| K_S^0 | data | 16236 \pm 127 | 23 \pm 5 | 116 \pm 11 | 124 \pm 11 |
| | MC | 16185 \pm 91 | 33 \pm 4 | 111 \pm 8 | 123 \pm 8 |
| K^\pm | data | 34952 \pm 187 | | 144 \pm 12 | 340 \pm 18 |
| | MC | 35075 \pm 134 | | 151 \pm 10 | 350 \pm 14 |
| high x_E | data | 49160 \pm 222 | | | 258 \pm 16 |
| | MC | 49245 \pm 159 | | | 273 \pm 12 |

| (b) | | N^{tag} | K_S^0 | K^\pm | high x_E |
|------------|------|------------------|------------|------------|--------------|
| K_S^0 | data | 3123 \pm 56 | 14 \pm 4 | 24 \pm 5 | 101 \pm 10 |
| | MC | 3118 \pm 40 | 19 \pm 3 | 23 \pm 3 | 113 \pm 6 |
| K^\pm | data | 8099 \pm 90 | | 2 \pm 1 | 197 \pm 14 |
| | MC | 7938 \pm 64 | | 0 | 190 \pm 9 |
| high x_E | data | 27909 \pm 167 | | | 419 \pm 20 |
| | MC | 27755 \pm 119 | | | 407 \pm 12 |

Table 2: Number of doubly tagged events when: (a) both tags belong to the lower x_E region, (b) at least one tag belongs to a higher x_E region. The upper rows are the measured data. The lower rows present the reweighted simulation data (MC). Also the total number of tags are given for data and the simulation (third column).

but δ was found to be consistent for all three tags. The impact of this reweighting on the flavour fractions is negligible and was considered as an additional systematic uncertainty in Section 5.

The flavour composition and its sensitivity to changes in the fragmentation function can be checked with measured data. To this end the number of events with a single and a double tag have been counted and compared in measured and simulated data following the proposal of [19]. Here a double-tagged event has exactly one tagged particle in each hemisphere, whereas single-tagged events have at least one tag. These counts depend on the sums and products of the flavour fractions. Due to the small number of tagging samples it is not possible to find a unique solution in this analysis. However, the single-tagged and double-tagged events can be used to cross-check the flavour fractions obtained from the Monte Carlo simulation using measured data only.

Double-tagged events were studied in different x_E ranges of the tagged particles. Each of the three samples was divided into two x_E regions. For each sample the lower x_E region was chosen so that the impact from the choice of the parameters of the fragmentation function is small. The remaining part corresponds to the higher x_E region which is particularly sensitive to the hardness of the fragmentation function. In detail, the lower x_E ranges were chosen for the K_S^0 and K^\pm samples to be $0.4 < x_E < 0.6$, and for the high x_E sample to be $0.6 < x_E < 0.7$. The higher x_E regions are $0.6 < x_E < 1.07$ for both kaon selections and $0.7 < x_E < 1.07$ for the high x_E sample. For both the lower and the higher x_E regions the number of double-tagged events were determined. The events were classified according to whether (a) both tags belong to the lower x_E region, or (b) at least one tag belongs to a higher x_E region. Table 2 lists the double tag counts for data

and simulation, normalized to the integrated luminosity of the data after the reweighting. Good agreement between the double tag counts in data and simulation is found for both x_E regions, as can be seen from Table 2. This can be quantified using the χ^2 per degree of freedom of the double tag counts which is 3.6/8 (5.3/8) in the higher (lower) x_E regions. Since the double tag counts depend on the flavour fractions, the good agreement for the absolute number of tags and for the number of double tags leads to the conclusion that the estimate of the flavour fractions by the JETSET generator is reliable.

Different multiplicities for events from primary u, d, or s quarks could imply different fragmentation functions for these quarks. To test the impact of different fragmentation functions another cross-check was conducted which considers a different reweighting factor $f(x_E) = c \cdot (1 - x_E)^\delta$ for one of the three light quarks. This corresponds to the case of a different fragmentation function for one quark flavour with respect to the other two. The flavour dependence was modelled by allowing in turn for a different value of δ for one of the three light quarks while maintaining as a constraint in the fit of the δ parameters the agreement of both the number of single tag counts and the x_E spectra in data and simulation as before.

When this reweighting was applied to the simulation, the light flavour fractions of the two kaon selections changed by less than 0.08, while for the high x_E selection the fractions changed by up to a factor of two. The comparison of the double tag counts after the flavour dependent reweighting revealed, however, a worse description of the data by the simulation than in the case of the flavour independent reweighting. This can be inferred from the χ^2 per degree of freedom for the number of double tag counts in the whole x_E regions considered which increased to 27.7/7, 13.7/7, or 36.5/7, respectively for each sample, when allowing for a different value of δ and, hence, a different fragmentation function for up, down, or strange quarks. These large values of χ^2 per degree of freedom strongly disfavour a flavour dependent reweighting of the fragmentation functions and, therefore, the substantial changes of the flavour fractions associated with this reweighting. This gives further evidence that the flavour fractions derived from the simulation can be considered to be an accurate estimate of the flavour fractions in the data. We, therefore, use for our main result the flavour fractions obtained from JETSET without application of the reweighting procedure. The small effect on the flavour fractions due to the reweighting will yield a systematic uncertainty which is discussed in Section 5.

4 Determination of charged particle multiplicities

4.1 Determination of flavour dependent multiplicities

The flavour dependent multiplicities are defined as the average number of charged particles with life-times $\tau > 300$ ps emerging from a decay of a Z into one of the three light quark flavours, u, d, or s, as for the inclusive multiplicities in [20]. To obtain these multiplicities from the charged particle tracks measured for each of the three selections, several corrections must be applied. In particular, the finite detector resolution and acceptance, and biases due to the tag selections must be accounted for.

The requirement of a high energy of the tagging particles in all three selections affects the multiplicity in its hemisphere due to a reduced phase space for the production of other particles. In the opposite hemisphere the effect is much smaller. This can be seen in Figure 2 where the mean charged particle multiplicities per hemisphere in the three selections are plotted in bins of the tagging particle's energy. To keep the bias of the multiplicity due to the tagging small we determine the multiplicities only in the hemispheres opposite to the tagged particles.

The remaining small dependence of the multiplicity in the opposite hemisphere on the energy of the tagging particle is due to the impact of the high energy of this particle. The higher the energy required of the leading particle the more the phase space is reduced, which is available for particle production, and, therefore, the mean charged multiplicity in the opposite hemisphere. It should also be noted from Figure 2 that the Monte Carlo simulation satisfactorily describes the effects in the opposite hemisphere due to the tag, although it tends to slightly overestimate the multiplicity in particular if the energy of the tagging particle is very high. This is due to a slight underestimation of the rate of badly reconstructed tracks in the simulation which particularly affects the hemisphere of the tagging particle if the measured energy fraction, x_E , of such a track is close to or above the physical limit of 1. Since the differential cross-section is tiny for leading particles with x_E close to 1, the effect of events selected due to badly reconstructed tracks on the mean charged multiplicity in the opposite hemisphere is negligible when considering the full range of x_E used for the tagging. Any remaining discrepancies between data and Monte Carlo simulation in the opposite hemisphere are taken as a source of systematic error, which is treated in Section 5.

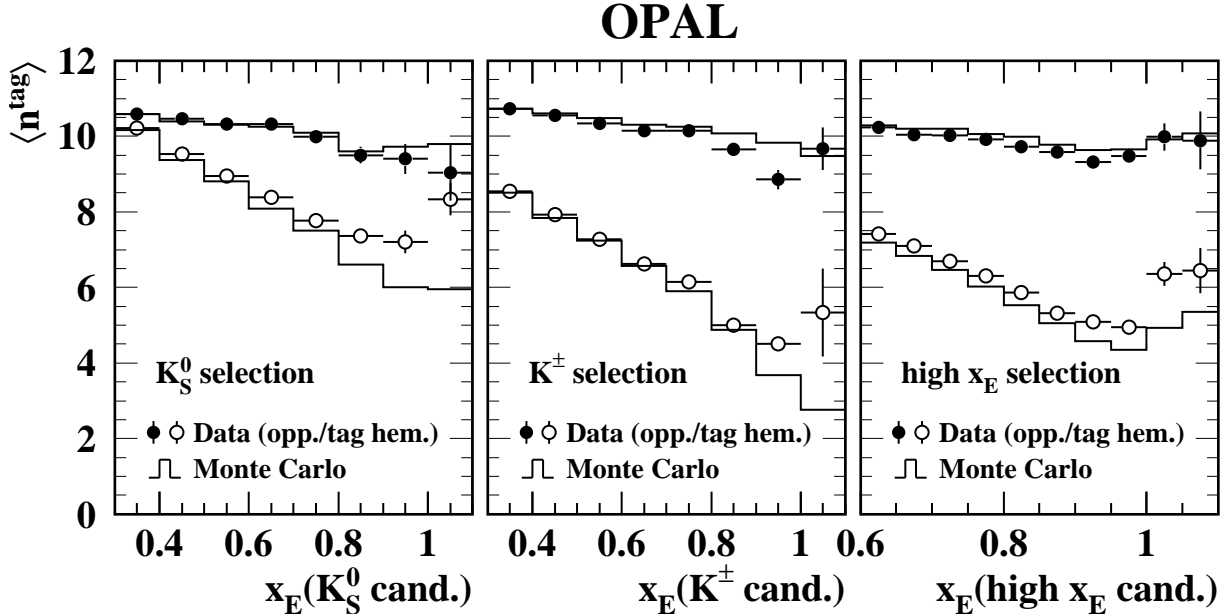


Figure 2: Mean charged multiplicity in a hemisphere as a function of the energy of the tagged particles. Open circles show the values obtained from the hemispheres containing the tagged particle, full circles correspond to the opposite hemispheres. The histogram is the expectation from the Monte Carlo simulation.

OPAL

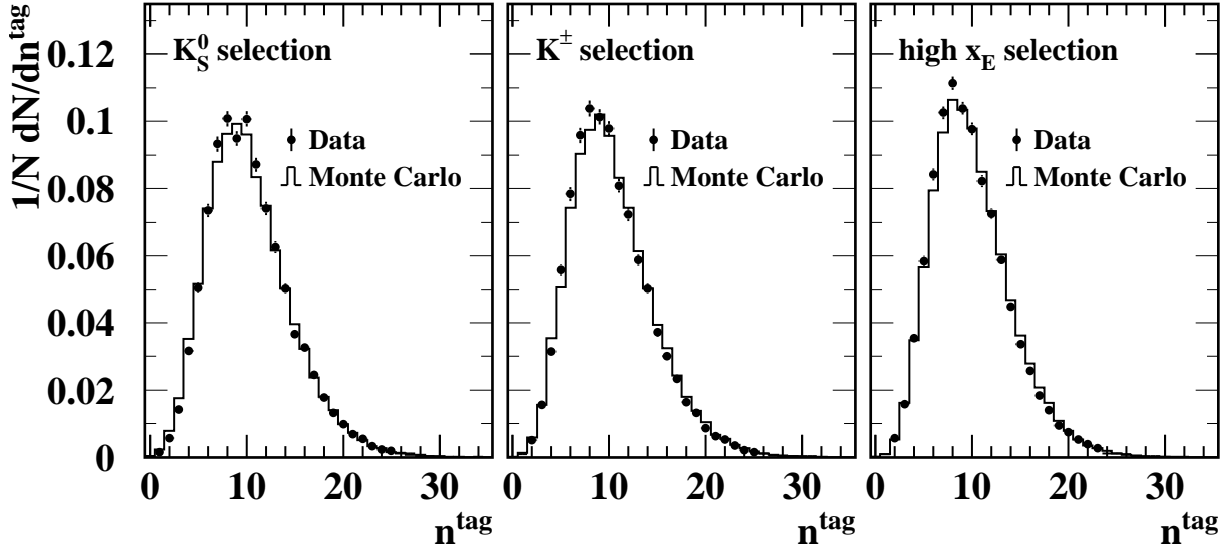


Figure 3: Charged multiplicity distributions of the three selections, measured in the hemispheres opposite to the tag particles. Overlaid are the expectations from the Monte Carlo simulation.

Figure 3 shows the multiplicity distributions and Table 3 lists the averages of the distributions for the hemisphere opposite to the tag. In the K_S^0 sample good agreement between data and the Monte Carlo is found, but in the events selected by a highly energetic K^\pm or high x_E tag the simulation predicts a slightly larger multiplicity.

4.2 Unfolding procedure

The three tag samples are composed of events with all five primary quark flavours accessible at LEP I. A statistical unfolding procedure was applied to obtain the mean charged particle multiplicities for each light quark flavour. The procedure simultaneously corrects for effects due to the selection cuts and for detector effects.

| | tag | K_S^0 | K^\pm | high x_E |
|----------|---|--------------------|--------------------|--------------------|
| Data | $\langle n^{\text{tag}} \rangle =$ | 10.373 ± 0.031 | 10.229 ± 0.031 | 9.883 ± 0.024 |
| MC udscb | $\langle n_{\text{MC}}^{\text{tag}} \rangle =$ | 10.323 ± 0.022 | 10.362 ± 0.021 | 10.031 ± 0.015 |
| MC u | $\langle n_{\text{u, MC}}^{\text{tag}} \rangle =$ | 10.171 ± 0.074 | 10.377 ± 0.045 | 10.089 ± 0.027 |
| MC d | $\langle n_{\text{d, MC}}^{\text{tag}} \rangle =$ | 10.187 ± 0.056 | 10.370 ± 0.059 | 9.995 ± 0.029 |
| MC s | $\langle n_{\text{s, MC}}^{\text{tag}} \rangle =$ | 10.119 ± 0.029 | 10.242 ± 0.029 | 9.921 ± 0.025 |
| MC c | $\langle n_{\text{c, MC}}^{\text{tag}} \rangle =$ | 10.853 ± 0.057 | 10.684 ± 0.070 | 10.314 ± 0.084 |
| MC b | $\langle n_{\text{b, MC}}^{\text{tag}} \rangle =$ | 11.932 ± 0.101 | 11.717 ± 0.147 | 11.660 ± 0.132 |

Table 3: Mean charged multiplicities and statistical errors of the three selections, measured in the hemispheres opposite to the tagged particles after applying the reweighting procedure described in Section 3.4.

| flavour q | mean multiplicity $\langle n_{q, \text{MC had.}} \rangle$ |
|-------------|---|
| u | 20.097 ± 0.005 |
| d | 19.987 ± 0.005 |
| s | 19.897 ± 0.005 |
| c | 21.387 ± 0.005 |
| b | 23.725 ± 0.005 |

Table 4: Mean generated charged multiplicities $\langle n_{q, \text{MC had.}} \rangle$ as obtained from the Monte Carlo generator JETSET 7.4. Only charged particles with life-times $\tau > 300$ ps were considered.

The measured mean charged multiplicities, $\langle n^{\text{tag}} \rangle$, in the hemisphere opposite to the tagged particle are expressed as

$$\langle n^{\text{tag}} \rangle = \sum_{q=u,d,s,c,b} f_q^{\text{tag}} \cdot \left[\frac{\langle n_{q, \text{MC}}^{\text{tag}} \rangle}{\langle n_{q, \text{MC had.}} \rangle} \right] \cdot \langle n_q \rangle \quad , \quad \text{tag} = K_S^0, K^\pm, \text{high } x_E \quad . \quad (1)$$

Here f_q^{tag} is the fraction of events with primary quark flavour q in a sample denoted by “tag”. It is listed in Table 1. The term in square brackets was also taken from the Monte Carlo simulation. It is the ratio of the mean charged multiplicity of the opposite hemisphere for events with primary quark flavour q in the “tag” sample, $\langle n_{q, \text{MC}}^{\text{tag}} \rangle$, listed in Table 3, and the number for both hemispheres obtained without detector simulation, $\langle n_{q, \text{MC had.}} \rangle$, which is given in Table 4. This ratio corrects (i) for the biases due to the tagging cuts, (ii) for the restriction to the hemisphere opposite to the tag particle when determining the charged multiplicity, and (iii) for effects from the selection of multihadronic events, the finite resolution and acceptance of the detector. On average the correction factor in square brackets is $1/(2 \times 1.007)$ for all flavours varying at most by $\pm 3.7\%$, and where the factor of 2 is due to considering a single hemisphere only for the determination of the multiplicities denoted by “tag”.

The flavour dependent mean charged multiplicities, $\langle n_q \rangle$, can be determined by solving the equation system (1). The values of $\langle n_c \rangle$ and $\langle n_b \rangle$ were taken from our previous determination [21]:

$$\langle n_c \rangle = 21.55 \pm 0.37 \pm 0.64 \quad (2)$$

$$\langle n_b \rangle = 23.16 \pm 0.02 \pm 0.45 \quad , \quad (3)$$

where the errors are statistical and systematic, respectively. The solution of the equation system (1) using the measured multiplicities in the hemisphere opposite to the tagging particles from Table 3 yielded

$$\langle n_u \rangle = 17.77 \pm 0.51$$

$$\langle n_d \rangle = 21.44 \pm 0.63$$

$$\langle n_s \rangle = 20.02 \pm 0.13$$

where the errors are statistical only. Combining these, and considering the statistical correlation matrix:

| | u | d | s |
|---|------|-------|-------|
| u | 1.00 | -0.90 | +0.06 |
| d | | 1.00 | -0.42 |
| s | | | 1.00 |

and using the branching ratios of $Z \rightarrow u\bar{u}$, $d\bar{d}$, $s\bar{s}$ from [22] one obtains $\langle n_{uds} \rangle = 19.90 \pm 0.09$ (stat.). This is in agreement within systematic errors with the results of [21, 23] which were obtained using a different method. The mean charged multiplicities $\langle n_u \rangle$ and $\langle n_d \rangle$ are almost fully anti-correlated, since the statistical separation power for u and d quarks is due to the small but different fractions of these quarks in the K_S^0 and the K^\pm samples.

4.3 Test of the unfolding procedure

It was checked that the unfolding procedure described in Section 4.2 is able to determine the flavour dependent multiplicities. For this test the Monte Carlo data sample was split into two disjoint parts. The smaller, comprising about the same statistics as the measured data, was used in place of the measured data which were to be corrected using the larger part of the Monte Carlo events. The multiplicities $\langle n_u \rangle = 20.05 \pm 0.63$ (stat.), $\langle n_d \rangle = 19.98 \pm 0.81$ (stat.), and $\langle n_s \rangle = 19.89 \pm 0.16$ (stat.) are in excellent agreement with the mean multiplicities obtained from the Monte Carlo generator (cp. Table 4).

5 Systematic study of the particle multiplicities

In addition to the consistency check based on the double tag rates in Section 3.4 and the test of the unfolding procedure in Section 4.3, many sources of systematic uncertainties were investigated which may be subdivided into five groups, namely (i) fluctuations due to limited Monte Carlo statistics, (ii) the experimental precision of the multiplicity in charm and bottom events, (iii) impacts of detector effects and event selection and the dependence of the mean charged multiplicity on the choice of the hadronization model, (iv) variations of tagging cuts, and finally, (v) impacts on the flavour fractions, f_q^{tag} , due to variations of hadronization parameters of the Monte Carlo generator, the matching of the Monte Carlo x_E spectra and hemisphere correlations to the data, and changes of the hadronization model. Apart from the items (i) and (ii), whose error contributions were estimated by error propagation, the general procedure to derive the uncertainty associated with the source was to repeat the complete analysis with one of the cuts or parameters varied. Any deviation from the result found for the standard set of cuts and parameters was interpreted as a systematic uncertainty.

The respective error contributions of the uncertainties derived for the groups (i) to (v) were quadratically added to estimate the total systematic uncertainties. The individual error contributions are listed in Table 5. In the following sections the sources (iii) to (v) of systematic uncertainties will be discussed in more detail.

| source of uncertainty | | $\Delta\langle n_u \rangle$ | $\Delta\langle n_d \rangle$ | $\Delta\langle n_s \rangle$ |
|--|--|--------------------------------------|--------------------------------------|--------------------------------------|
| data statistics | | $\pm\mathbf{0.51}$ | $\pm\mathbf{0.63}$ | $\pm\mathbf{0.13}$ |
| MC statistics | | ± 0.37 | ± 0.48 | ± 0.09 |
| c, b multiplicity [21] | | ± 0.27 | ± 0.13 | ± 0.19 |
| detector [20] | | ± 0.17 | ± 0.20 | ± 0.19 |
| all | x_E -cut variation | -0.16 $+0.49$ | -0.79 $+0.35$ | $+0.22$ -0.10 |
| | $x_E < 0.9$ | -0.06 | -0.06 | $+0.02$ |
| K_S^0 | K_S^0 mass window | -0.24 | $+0.22$ | $+0.04$ |
| K^\pm | $ \cos\theta_{K^\pm} < 0.6, 0.8$ | ± 0.14 | ∓ 0.20 | ± 0.04 |
| | $N_{CJ} > 80, N_{dE/dx} > 80$ | $+0.09$ | -0.14 | $+0.02$ |
| | $N_{dE/dx} > 110$ | -0.15 | $+0.22$ | -0.04 |
| | $ w_{K^\pm} \geq 0.5, w_p > 0.4, w_{\pi^\pm} > -0.06$ | $+0.16$ | -0.23 | $+0.04$ |
| high x_E | $ \cos\theta_{\text{high } x_E} < 0.6, 0.8$ | $+0.01$ -0.01 | $+0.11$ -0.16 | $+0.05$ -0.03 |
| | $N_{CJ} > 120, 140$ | < 0.01 | $+0.03$ -0.01 | ∓ 0.01 |
| | $\chi_{r\varphi}^2 < 1.5$ | $+0.01$ | $+0.11$ | -0.03 |
| | selection cuts total | $+0.54$ -0.36 | $+0.53$ -0.88 | $+0.24$ -0.12 |
| $\Lambda_{LLA} = 250 \pm 6 \text{ MeV}$ | | ± 0.04 | ± 0.06 | ± 0.01 |
| $Q_0 = 1.9 \pm 0.5 \text{ GeV}$ | | ± 0.03 | ± 0.05 | ± 0.03 |
| $\sigma_q = 0.40 \pm 0.03 \text{ GeV}$ | | ± 0.04 | ± 0.05 | ± 0.01 |
| $b = 0.52^{+0.40}_{-0.26}$ | | -0.06 $+0.12$ | $+0.22$ -0.20 | $+0.04$ -0.09 |
| $\varepsilon_c = 0.031 \pm 0.011$ | | ± 0.06 | ± 0.06 | ± 0.05 |
| $\varepsilon_b = 0.0038 \pm 0.0010$ | | ± 0.06 | ± 0.11 | ± 0.02 |
| $\gamma_s = 0.31 \pm 0.10$ | | $+0.30$ -0.68 | -0.34 $+0.74$ | $+0.06$ -0.07 |
| $(u/s)/(d/s) = 0.45 \pm 0.04$ | | ± 0.03 | ± 0.06 | ± 0.02 |
| $V_{d,u} = 0.60 \pm 0.10$ | | ± 0.04 | ± 0.07 | ± 0.02 |
| $V_s = 0.40 \pm 0.05$ | | -0.36 $+0.26$ | $+0.39$ -0.31 | -0.04 $+0.03$ |
| no tensor mesons | | -0.58 | $+0.85$ | -0.14 |
| $B(c \rightarrow K_S^0 + X) : \pm 13.9 \% \oplus B(b \rightarrow K_S^0 + X) : \pm 10.0 \%$ | | ± 0.14 | ∓ 0.13 | ∓ 0.02 |
| $B(c \rightarrow K^\pm + X) : \pm 11.5 \% \oplus B(b \rightarrow K^\pm + X) : \pm 21.6 \%$ | | ∓ 0.07 | ± 0.10 | ± 0.02 |
| reweighted x_E spectra | | -0.35 | $+0.17$ | -0.03 |
| hemisphere correlations | | -0.01 | $+0.02$ | < 0.01 |
| hadronization total | | $+0.46$ -1.05 | $+1.25$ -0.56 | $+0.11$ -0.20 |
| total systematic errors | | $+\mathbf{0.86}$ $-\mathbf{1.20}$ | $+\mathbf{1.46}$ $-\mathbf{1.17}$ | $+\mathbf{0.39}$ $-\mathbf{0.37}$ |
| total errors | | $+\mathbf{1.01}$ $-\mathbf{1.31}$ | $+\mathbf{1.59}$ $-\mathbf{1.33}$ | $+\mathbf{0.41}$ $-\mathbf{0.40}$ |

Table 5: Compilation of individual contributions to the total error.

5.1 Uncertainties from detector simulation and event selection

The detector simulation was needed to correct for the fraction of multiplicity that was not recorded by the detector either owing to limited acceptance, biases of the event selection, or interactions in the detector such as δ -electrons or hadronic interactions, all of which have been studied in great detail in [20]. In total an error of about 1 % due to this source of systematic uncertainty was estimated in [20]. This was also adopted for this measurement.

5.2 Uncertainties from tagging

The measured multiplicity depends on the energy of the tagged particle. Although this effect is reduced by measuring the multiplicity in the hemisphere opposite to the tag residual effects have to be taken into account.

- Variations of the x_E cuts in steps of 0.05 by as much as ± 0.1 around the default cut value were done. The largest up- and downward excursions yielded the error estimates for the multiplicities.
- Also a more stringent cut on the maximum accepted momentum, $x_E < 0.9$, for all tags did not change the measured multiplicities by more than 0.4 %.

For each of the three tag types the impact of the choice of the most important selection cuts was studied.

- For the K_S^0 the allowed mass window around the world average mass value [17] was altered from 120 MeV within the range of 80 to 200 MeV.

Since the K^\pm selection relies very much on the capability to precisely measure the energy loss in the jet chamber, the relevant cuts were investigated.

- As the precision of the measurement of dE/dx degrades towards the very forward and backward regions, the $|\cos \theta_{K^\pm}| < 0.72$ requirement was varied in small steps between 0.6 and 0.8, taking the r.m.s. to estimate the contribution to the systematic uncertainty.
- The minimum number of both jet chamber hits and dE/dx hits was relaxed from 130 to 80.
- The required number of dE/dx hits was increased from 100 to 110.
- From the various modifications to the energy loss weight cuts, namely choosing a tighter cut on the kaon dE/dx weight of 0.5 instead of 0.1, adding an additional rejection cut on the proton dE/dx weight of 0.4, or considering a better pion rejection by requiring its dE/dx weight to be larger than -0.06 , only the first one contributes a significant systematic error.

The high x_E selection critically depends on the ability of the jet chamber to reliably measure high momentum particles.

- As for K^\pm , the allowed range of $|\cos\theta_{\text{high } x_E}|$ was varied from less than 0.72 to either less than 0.6 or 0.8.
- A variation of the minimum number of hits required for a high x_E particle in the jet chamber by ± 10 around the standard value of 130 had only a negligible effect on all flavours.
- Tightening the cut on the $\chi^2_{r\varphi}$ of the track fit from 2 to 1.5 affected the multiplicity by less than 0.5 %.

5.3 Uncertainties due to impacts on flavour fractions

The Monte Carlo event generator requires several parameters to be adjusted for a proper description of the measured data. Changing these hadronization parameters affects the flavour composition, f_q^{tag} , and, therefore, tests the sensitivity of the result of this analysis on the particular choice of these parameters. In the following we consider those parameters which are expected to have an impact on the flavour fractions. These were varied about their tuned values within the intervals quoted in [14] apart from the b and γ_s parameters where larger variations were investigated, in particular the range for γ_s given in [24]. Most of the parameter variations did not significantly affect the flavour dependent multiplicities, $\langle n_{q, \text{MC had.}} \rangle$, or the flavour fractions, f_q^{tag} , of Eq. (1). We therefore mention only the significant changes of the flavour fractions due to the parameter variations.

- The amount of gluon radiation was modified by varying the Λ_{LLA} parameter and the cut-off of the parton shower, Q_0 .
- During the hadronization step a hadron receives extra transverse momentum whose size is controlled by the parameter σ_q which was changed from its tuned value.
- The fraction of energy and momentum transferred from a heavy c or b quark to the related hadron also has an impact on the background contributions from these heavy quarks. The relevant ε parameters of the Peterson et al. [25] fragmentation function were varied. Only the change of ε_c , except for the charm quark fraction itself, had a noticeable effect on the strange quark fraction of about -0.01 to $+0.005$ for the two kaon selections.
- To account for a remaining uncertainty from the hardness of the light quark fragmentation functions despite the impact of the reweighting procedure, the parameter b of the Lund symmetric fragmentation function in JETSET was varied in several steps in the range of 0.26 to 0.92. This changed in particular the strange quark fraction in the range of -0.06 to $+0.04$ for the K_S^0 and in the range of -0.04 to $+0.03$ for the K^\pm selection. The u and d fractions varied owing to this variation of b by ± 0.012 at most in all three selections.

- Since the statistical separation between u and d quarks is based on the K_S^0 and K^\pm production, the relative amount of $s\bar{s}$ quark pairs created from the vacuum, γ_s , was changed in steps in the range of 0.21 to 0.41 [24]. This led to changes of the light quark fractions in the K^\pm (K_S^0) selection ranging from -0.05 , -0.03 , $+0.06$ (-0.02 , -0.03 , $+0.04$) to $+0.06$, $+0.02$, -0.05 ($+0.01$, $+0.02$, -0.04), respectively, for u, d, s quarks. For the high x_E selection only changes of the u and s quark fractions were observed at a level of ± 0.01 .
- For baryons with strangeness an extra suppression factor $(u/s)/(d/s)$ exists in JETSET whose variation resulted in only negligible changes of both the flavour composition and the flavour dependent multiplicities.
- The production of vector mesons was considered. Although the down and strange quark fractions of the high x_E selection changed by about ± 0.02 , the relative portion $V_{u,d}$ of vector mesons from u and d quarks was of minor importance for the flavour dependent multiplicities.
- The fraction of vector mesons from s quarks, V_s , substantially affects the yields of leading K_S^0 and K^\pm mesons. The variation of this parameter mostly changed the fraction from up and down quarks in the K^\pm selection by about ± 0.01 , and at the same level also that from down and strange quarks of the high x_E selection. Since the statistical u-d quark separation strongly relies on the u and d quark fractions in the two kaon selections, a change of this parameter led to a large error contribution as can be seen from Table 5.
- Similarly, the decay products of tensor mesons have a softer x_E spectrum. However, the yields of these are not well known. Thus, the impact was estimated by analyzing about 3.5 million fully simulated events from the JETSET generator tuned to describe the data, but without the production of tensor mesons. This yielded a substantial reduction of the strange quark fraction by -0.025 in the K_S^0 , -0.035 in the K^\pm , and -0.065 in the high x_E selections. The up and down quark fractions in the K_S^0 and K^\pm selections changed by -0.01 and -0.005 , whereas the d quark fraction in the high x_E selection increased by about $+0.03$. Thus the d and s quark fractions in the high x_E selection are about equal if tensor mesons do not contribute. The difference in the results with simulated tensor mesons is assigned as a systematic error.
- The uncertainty of the inclusive branching ratios of charm and bottom to K_S^0 and K^\pm was considered. From the data in [17] the relative errors on the $B(c \rightarrow K_S^0 X, K^\pm X)$ branching ratios have been determined to be $\pm 11.5\%$, $\pm 13.9\%$, and on $B(b \rightarrow K_S^0 X, K^\pm X)$ to be $\pm 21.6\%$, $\pm 10.0\%$, respectively. Their impact on the flavour dependent multiplicities was assessed by varying the charm and bottom contributions in the K_S^0 and K^\pm tagged event samples according to these percentages.
- To account for the poor simulation of the x_E spectra of the tagged particles in the tuned Monte Carlo the reweighting functions of Section 3.4, $f(x_E) = c \cdot (1 - x_E)^\delta$, were employed. Applying these specific reweighting functions to all three selections resulted in a small reduction of the strange quark fraction by 1 to 2% while the

heavy quark contribution is increased accordingly. Moreover, it leads to an anti-correlated change of the order of 1 to 3 % of the u and d quark fractions but in opposite directions for the K_S^0 and the K^\pm event samples. The final multiplicities of u and d quarks change by up to 2 %.

- Finally, the small discrepancies between simulation and data noticed in the correlations of the opposite hemispheres shown in Figure 2 were considered. Depending on the x_E of the tagged particle the Monte Carlo events were reweighted to match the data. This had only a negligible effect on both the flavour fractions and the flavour dependent multiplicities changing them by less than 0.1 %.

In addition to the JETSET Monte Carlo event generator also the HERWIG program [26] was examined. While HERWIG yields a good description of the shape of the x_E spectra of the tagged particles, it does not reproduce the absolute rates. For instance, HERWIG predicts a much larger contribution to the high x_E sample from d quarks and less from u quarks due to a larger number of protons produced in HERWIG. Since the HERWIG expectation of the total proton yield is not in agreement with the measurements [17, 27], one might suspect that the flavour fractions obtained from this Monte Carlo generator are not reliable. Thus, no systematic error contribution from using HERWIG is quoted.

6 Cross-check with flavour fractions derived from double tag counts

The flavour fractions, f_q^{tag} , can be derived from data only using the number of single and double tag counts since they are related to the sum and products of flavour fractions [19]. The non-linearity of the equation system requires for its solution more than the six relations which are given by the numbers of single and double tags considered in this analysis even when the heavy flavour contributions are kept fixed.

Such an investigation has been done in [8] using the single and double tag counts of charged pions, kaons, protons, K_S^0 and Λ for $x_E > 0.4, 0.5$, and 0.6 . This analysis yielded the flavour dependent production rates of these hadrons where only the SU(2) isospin flavour symmetry and the flavour independence of the strong interaction were assumed for the production of charged pions, and charged and neutral kaons.

To compare with the results from [8], the flavour fractions, f_q^{tag} , were calculated from the quoted production rates neglecting correlations for this cross-check. The calculation took into account that these rates had been corrected for mis-identification of the tagging particle. The high x_E sample was approximated by adding the production rates of the charged particles, i.e. pions, kaons, and protons. The comparison of the flavour fractions at an x_E -cut of 0.4 for K_S^0 , 0.5 for K^\pm and 0.6 in the case of the high x_E sample revealed some substantial differences with respect to the JETSET prediction. The K_S^0 fraction from up quarks is 0.4 times and that from down quarks 1.7 times the value obtained from

the Monte Carlo simulation used for this analysis. The up quark contribution to the K^\pm sample is 1.23 times higher, while that of down quarks is about 0.75 times that obtained from the simulation. The fraction of high x_E particles originating from up quarks is about 10 % less than expected from the simulation. The strange quark fractions agree within ± 0.02 for each tagged event sample. These changes in the up and down quark flavour fractions are considerably larger than what was found from the variation of the JETSET parameters in Section 5.3.

Although the analysis in [8] explicitly assumed flavour independence of the strong coupling and SU(2) isospin symmetry, the flavour fractions obtained from [8] were used for the unfolding procedure described in Section 4.2 as a cross-check of the results. This yielded changes of the flavour dependent multiplicities of $\Delta\langle n_u \rangle = +0.60$, $\Delta\langle n_d \rangle = -1.41$, and $\Delta\langle n_s \rangle = +0.32$. Since these changes are essentially covered by the systematic errors discussed in Section 5 they are not considered as an additional systematic uncertainty.

7 Results

Adding the individual contributions to the systematic uncertainty from Monte Carlo statistics, the mean charged multiplicity in c and b quark events, the correction of detector acceptance and resolution, the selection cuts, and the parameters of the hadronization model in quadrature, the total systematic error of the flavour dependent mean charged multiplicities is about $\pm 7\%$ for up and down, and $\pm 2\%$ for strange quark events. The final results are

$$\begin{aligned}\langle n_u \rangle &= 17.77 \pm 0.51 \text{ (stat.) } {}^{+0.86}_{-1.20} \text{ (syst.)} \\ \langle n_d \rangle &= 21.44 \pm 0.63 \text{ (stat.) } {}^{+1.46}_{-1.17} \text{ (syst.)} \\ \langle n_s \rangle &= 20.02 \pm 0.13 \text{ (stat.) } {}^{+0.39}_{-0.37} \text{ (syst.)} .\end{aligned}$$

All errors apart from selection cuts, detector effects, and hadronization models were obtained by error propagation and, therefore, obey the statistical correlation as quoted in Section 4.2. The correlation coefficients for the remaining two groups of systematic uncertainties were determined separately for each individual systematic variation.

These flavour dependent mean charged multiplicities agree within the total errors, even though deviations may be expected due to decays of hadrons. For instance, the decay of the $\phi(1020)$ to charged kaons is enhanced over the decay to neutral kaons. Thus, the results from the JETSET generator displayed in Table 4 show a 1% spread between the charged multiplicities from up and strange quark events.

Some of the flavour dependent mean charged multiplicities are strongly correlated which must be considered when comparing the results. Taking these statistical and systematic correlations into account the ratios of the multiplicities are

$$\frac{\langle n_u \rangle}{\langle n_d \rangle} = 0.829 \pm 0.047 \text{ (stat.) } {}^{+0.081}_{-0.109} \text{ (syst.)} ,$$

$$\frac{\langle n_s \rangle}{\langle n_d \rangle} = 0.934 \pm 0.030 \text{ (stat.) } {}^{+0.062}_{-0.089} \text{ (syst.)},$$

$$\frac{\langle n_s \rangle}{\langle n_u \rangle} = 1.127 \pm 0.033 \text{ (stat.) } {}^{+0.057}_{-0.077} \text{ (syst.)},$$

which are all close to unity.

8 Summary and conclusions

A measurement of the charged multiplicity in events of u, d, and s quarks from e^+e^- annihilation at the Z pole is presented. Exploiting the leading particle effect to identify the primary quark flavour, samples of events differently enriched in u, d, and s were selected by tagging highly energetic K_S^0 , K^\pm and charged particles. The multiplicities per light quark flavour were obtained from a statistical unfolding of the multiplicities measured in the hemispheres opposite to the tagged particles. Hemisphere correlations were observed, but were found to be small and well-described by the Monte Carlo simulation. The final corrected multiplicities were determined to be

$$\langle n_u \rangle = 17.77 \pm 0.51 \text{ (stat.) } {}^{+0.86}_{-1.20} \text{ (syst.)}$$

$$\langle n_d \rangle = 21.44 \pm 0.63 \text{ (stat.) } {}^{+1.46}_{-1.17} \text{ (syst.)}$$

$$\langle n_s \rangle = 20.02 \pm 0.13 \text{ (stat.) } {}^{+0.39}_{-0.37} \text{ (syst.)},$$

where the $\langle n_u \rangle$ and $\langle n_d \rangle$ multiplicities are highly statistically anti-correlated (about -90%). The ratios of pairs of these multiplicities which take the correlations into account are all close to unity. This agrees with the expectation of QCD that the charged particle multiplicities are flavour independent for the light up, down, and strange quarks apart from small effects due to particle decays.

Acknowledgements:

We particularly wish to thank the SL Division for the efficient operation of the LEP accelerator at all energies and for their continuing close cooperation with our experimental group. We thank our colleagues from CEA, DAPNIA/SPP, CE-Saclay for their efforts over the years on the time-of-flight and trigger systems which we continue to use. In addition to the support staff at our own institutions we are pleased to acknowledge the Department of Energy, USA, National Science Foundation, USA, Particle Physics and Astronomy Research Council, UK, Natural Sciences and Engineering Research Council, Canada, Israel Science Foundation, administered by the Israel Academy of Science and Humanities, Minerva Gesellschaft, Benozziyo Center for High Energy Physics, Japanese Ministry of Education, Science and Culture (the Monbusho) and a grant under

the Monbusho International Science Research Program,
 Japanese Society for the Promotion of Science (JSPS),
 German Israeli Bi-national Science Foundation (GIF),
 Bundesministerium für Bildung und Forschung, Germany,
 National Research Council of Canada,
 Research Corporation, USA,
 Hungarian Foundation for Scientific Research, OTKA T-029328, T023793 and OTKA F-023259.

References

- [1] ALEPH Coll., D. Buskulic et al., Phys. Lett. **B355** (1995) 381;
 ALEPH Coll., R. Barate et al.: *A Measurement of the b -quark Mass from Hadronic Z Decays*, CERN-EP-2000-093, subm. to. Eur. Phys. J. **C**;
 DELPHI Coll., P. Abreu et al., Phys. Lett. **B307** (1993) 221;
 DELPHI Coll., P. Abreu et al., Phys. Lett. **B418** (1998) 430;
 L3 Coll., B. Adeva et al., Phys. Lett. **B271** (1991) 461;
 OPAL Coll., R. Akers et al., Z. Phys. **C65** (1995) 31;
 OPAL Coll., G. Abbiendi et al., Eur. Phys. J. **C11** (1999) 643;
 SLD Coll., K. Abe et al., Phys. Rev. **D53** (1996) 2271;
 SLD Coll., K. Abe et al., Phys. Rev. **D59** (1999) 012002.
- [2] OPAL Coll., R. Akers et al., Z. Phys. **C60** (1993) 397.
- [3] Yu.L. Dokshitzer, S.I. Troyan, in Proc. of the *XIX Winter School of the LNPI*, Vol. 1, Leningrad (1984) 144;
 Ya.I. Azimov, Yu.L. Dokshitzer, V.A. Khoze, S.I. Troyan, Z. Phys. **C27** (1985) 65.
- [4] B.R. Webber, Phys. Lett. **B143** (1984) 501;
 Yu.L. Dokshitzer, V.A. Khoze, A.H. Mueller, S.I. Troyan, *Basics of Perturbative QCD*, Edition Frontières, Gif-sur-Yvette, 1991.
- [5] DELPHI Coll., W. Adam et al., Z. Phys. **C69** (1996) 561;
 DELPHI Coll., P. Abreu et al.: Phys. Lett. **B479** (2000) 118;
 OPAL Coll., R. Akers et al., Phys. Lett. **B352** (1995) 176;
 SLD Coll., K. Abe et al., Phys. Rev. Lett. **72** (1994) 3145;
 SLD Coll., K. Abe et al., Phys. Lett. **B386** (1996) 475;
 VENUS Coll., K. Okabe et al., Phys. Lett. **B423** (1998) 407.
- [6] R.P. Feynman, R.D. Field, Nucl. Phys. **B136** (1978) 1;
 TASSO Coll., R. Brandelik et al., Phys. Lett. **B100** (1981) 357.
- [7] SLD Coll., K. Abe et al., Phys. Rev. Lett. **78** (1997) 3442, Erratum: *ibid.* **79** (1997) 959.
- [8] OPAL Coll., G. Abbiendi et al., Eur. Phys. J. **C16** (2000), 407.

- [9] OPAL Coll., K. Ahmet et al., Nucl. Instr. and Meth. **A305** (1991) 275.
- [10] O. Biebel et al., Nucl. Instr. and Meth. **A323** (1992) 169;
M. Hauschild et al., Nucl. Instr. and Meth. **A314** (1991) 74.
- [11] OPAL Coll., G. Alexander et al., Z. Phys. **C52** (1991) 175.
- [12] OPAL Coll., G. Alexander et al., Z. Phys. **C72** (1996) 191.
- [13] T. Sjöstrand, Comp. Phys. Comm. **82** (1994) 74.
- [14] OPAL Coll., G. Alexander et al., Z. Phys. **C69** (1995) 543.
- [15] J. Allison et al., Nucl. Instr. and Meth. **A317** (1992) 47.
- [16] OPAL Coll., G. Alexander et al., Phys. Lett. **B264** (1991) 467.
- [17] C. Caso et al., Eur. Phys. J. **C3** (1998) 1.
- [18] B. Andersson, G. Gustafson, G. Ingelman, T. Sjöstrand, Phys. Rep. **97** (1983) 33.
- [19] J. Letts and P. Mättig, Z. Phys. **C73** (1997) 217.
- [20] OPAL Coll., R. Akers et al., Z. Phys. **C68** (1995) 203.
- [21] OPAL Coll., K. Ackerstaff et al., Eur. Phys. J. **C7** (1999) 369.
- [22] D. Bardin et al., *ZFITTER: An Analytical Program for Fermion Pair Production in e^+e^- Annihilation*, CERN-TH. 6443/92, hep-ph/9412201;
D. Bardin et al., Phys. Lett. **B255** (1991) 290;
D. Bardin et al., Nucl. Phys. **B351** (1991) 1;
D. Bardin et al., Z. Phys. **C44** (1989) 493.
- [23] OPAL Coll., K. Ackerstaff et al., Eur. Phys. J. **C1** (1998) 479.
- [24] A. Blondel et al., in *Physics at LEP 2*, Vol. 2, G. Altarelli, T. Sjöstrand, F. Zwirner (eds.), CERN 96-01.
- [25] C. Peterson et al., Phys. Rev. **D27** (1983) 105.
- [26] G. Marchesini et al., Comp. Phys. Comm. **67** (1992) 465.
- [27] R.J. Hemingway, in Proc. of the *XXVII Int. Conf. High Energy Physics*, P.J. Bussey, I.G. Knowles (eds.), Institute of Physics Publishing (IOP), Bristol;
I.G. Knowles and G.D. Lafferty, J. Phys. **G23** (1997) 731;
M.G. Green, S.L. Lloyd, P.N. Ratoff, D.R. Ward, *Electron Positron Physics at the Z*, Institute of Physics Publishing (IOP), Bristol.